JOURNAL OF MATERIALS SCIENCE 5 (1970) 425–433

Neutron-Induced Autoradiography of Lithium Silicate Glasses

F. W. WOOD
Albany Metallurgy Research Center, US Department of the Interior, Bureau of Mines, Albany, Oregon, USA
A. H. ROBINSON
Radiation Center, Oregon State University, Corvallis, Oregon, USA

Immiscibilities between silica and lithium disilicate were investigated. Alpha particles ejected from ^{6}Li atoms by thermal neutrons were used to autoradiograph surfaces representing diffusion-zone cross-sections. Etchant-enlarged alpha tracks in nitrocellulose disclosed the distribution of lithium. For autoradiography, procedural details were established, suitable operating conditions were selected, and the method was calibrated. For diffusion, adequate couples had to be prepared. Subsequent experiments indicated phase separations along an 885° C isotherm of the silica-lithium disilicate system. There was evidence of metastable compositions near 30, 25, 20, 16, 11, and 7 mol % of lithia in silica. These results have been given a very tentative interpretation: The first two compositions may correspond to metastable extensions of liquidus boundaries, projected through a eutectic point of the system. The third and sixth compositions are probably points on a liquid-liquid miscibility boundary, and the fourth and fifth compositions could be on an associated spinodal boundary.

1. Introduction

An investigation of the microstructural miscibility of lithia in silica was used as an exploratory and developmental, but also purposeful application of an autoradiographic procedure depending on the ejection of alpha particles from ^{6}Li atoms by thermal neutrons. The general approach was to form various phases containing up to about 33 mol % of lithia in silica by diffusing lithium disilicate, $Li_2O \cdot 2SiO_2$, and silica, SiO_2, together, then to distinguish the phases compositionally by means of neutron-induced autoradiography of a surface exhibiting the diffusion profile.

The use of autoradiography as a tool for metallography, ceramography, and petrography is a recent development. In essence, microscopic heterogeneities at a surface are mapped by detecting characteristic particles or electromagnetic radiation emitted by some atomic or molecular constituent of the surface because of either spontaneous activity or an external stimulus. In various cases on record, the emissions have included alpha particles [1, 2], beta particles [3], and massive fission fragments [4, 5], and where external stimulation was involved, it has been provided by thermal neutrons. Actually, an electron microprobe operated in an X-ray or secondary-electron mode, a secondary-electron spectrometer, and an Auger-electron spectrometer are examples of systems that utilise similar principles, although they are not generally classed as autoradiographic and are characterised by extranuclear interactions of particles. Studies of oxide layers on metals by observing the nuclear scattering of protons [6], ^{3}He particles [7] and deuterons [8] also are basically related.

Typically, an autoradiographic detector is either a photographic emulsion [3] or a dielectric material placed in intimate contact with the surface to be studied [9] so that particles ejected from the surface leave characteristic tracks in the dielectric detector. The former type of detector cannot be exposed to radiation in a reactor. In the dielectric detectors, tracks are normally too small for optical observation [10] but they can be made visible at reasonable magnifications by using an etchant that pre-

ferentially attacks and enlarges the damaged sites [11, 12]. When alpha particles are the tracking particles, it has been shown [1, 2, 13] that cellulose nitrate and sodium hydroxide are a good detector-etchant pair. Furthermore, the behaviour of cellulose nitrate in this service has been studied in some detail [14].

2. Development of Procedures

2.1. Autoradiography

The distribution of lithium at a solid surface is detected autoradiographically by means of the reaction $^{6}Li(n,\alpha)^{3}H$ in which thermal neutrons are captured. The capture cross-section is about 910 barns, and the natural abundance of ^{6}Li is about 7.5%. Liberated alpha particles interact strongly with matter and have a short range. Thus, only those originating within a few molecular layers of the surface can emerge, and these are capable of only shallow penetration into a dielectric detector. The pattern of damage in the detector closely corresponds to the distribution of lithium at the specimen surface.

The basic procedure used for autoradiography was to prepare a specimen surface by grinding and polishing, then to place it in firm contact with a piece of cellulose nitrate sheet while both the specimen and detector were irradiated with thermal neutrons in the Oregon State University TRIGA-III research reactor. Appropriate irradiation levels are in the orders of 10^{9} and 10^{10} neutrons cm^{-2}. In this work, the number of neutrons was controlled indirectly by controlling reactor energy (product of power and time), but it probably would have been better to monitor the neutron exposure of specimens directly. After irradiation, plastic film was developed by etching in a 6N solution of NaOH at room temperature. Commercially produced cellulose nitrate sheet was used. It was much thicker, at about 900 μm, than necessary, and it contained about 25% of synthetic camphor as a solvent plasticiser and traces of an alcohol secondary solvent, in addition to nitrocellulose. The material retained latent tracks for several weeks without apparent difficulty. Neutron irradiations were accomplished in the "lazy-susan" irradiation rack of the TRIGA-III reactor. Specimens and 2-cm discs of the cellulose nitrate were mounted in special aluminium holders for the irradiation. Each specimen was pressed against the plastic by a coiled spring of zirconium.

In order to associate ranges of composition with separate phases, a quantitative calibration relating densities of alpha tracks with lithium content was needed. This requirement was facilitated by the availability of the glasses listed in table I. They were prepared as a part of some earlier work [15]. The lithia contents were determined by photometric analyses. Apparent discrepancies of combined silica and lithia are due mainly to inaccuracies of wet analyses for silica. Contamination, including Al, Cu, Fe, Mg, Na, and Ti, was less than 0.5 wt% in each case. A calibration experiment comprised autoradiography of a set of the "standard" specimens at a selected irradiation energy, whereby etched plastic was examined at $\times 400$, alpha tracks were counted visually, and the track density was correlated with lithia content.

Initially, calibrations were attempted at reactor energies of about 40 kW-sec, 25 kW-sec and 10 kW-sec. Useful results were obtained only at the low energy. At the higher energies, the areal densities of tracks in the detectors were high and there was excessive superposition of tracks. Consequently, track counts were generally too low, and the apparent calibrations were non-linear and non-reproducible. An example of the autoradiographs obtained is shown in fig. 1. At the nominal energy of 10 kW-sec, the calibration was essentially linear, having a gradient of 9×10^{6} tracks/cm^{2}/mol fraction Li_2O. The nominal energy ultimately selected for use in experiments was 3 kW-sec, and the calibration gradient at this level was 2.7×10^{6} tracks/cm^{2}/mol fraction Li_2O. It is implicit in these results that the calibration gradient changes linearly with irradiation energy, at least for energies up to about 10 kW-sec. Fig. 2 is an example of an autoradiograph at

TABLE I Lithia-silica glass specimens used for calibration

Code symbol	Wt % SiO_2	Wt % Li_2O	Mol % SiO_2	Mol % Li_2O	$Li_2O{\cdot}2SiO_2$
H3	77.9	20.2	63.8	33.6	~100
H4	80.5	19.0	67.4	31.9	95.7
H5	81.5	17.2	68.8	29.3	87.9
H6	87.3	11.8	77.5	21.1	63.3

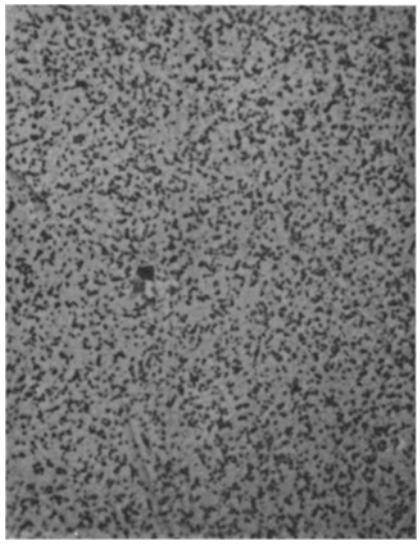

Figure 1 Autoradiograph of vitreous lithium disilicate, resulting from 25 kW-sec thermal neutron irradiation. Unmagnified alpha track density is about 6×10^6 cm^{-2}.

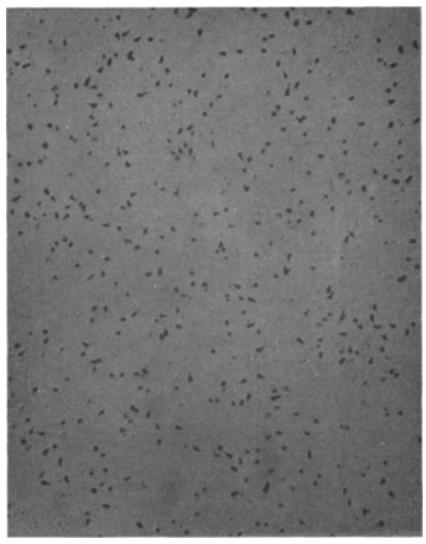

Figure 2 Autoradiograph of silica glass containing about 30 mol % lithia, resulting from 3 kW-sec thermal neutron irradiation. Unmagnified alpha track density is about 8×10^5 cm^{-2}.

a low irradiation energy.

A problem in achieving calibration was inconsistent etching times. The times required to develop all tracks in a detector varied from 60 to 150 min. That is, after these times, additional etching only enlarged the pits without revealing new evidence of tracks. Shorter and more predictable developing times would certainly be advantageous, and in retrospect it seems that the developing should have been done in a controlled-temperature bath at about 60° C rather than at room temperature.

Another matter of concern was the accuracy of track counting. Both the neutron-alpha reaction and the alpha-tracking process are statistical in nature, and they are subject to normal dispersion even under ideal conditions. But in addition, currently practicable counting techniques involve an appreciable degree of human judgement, with a high risk of introducing error. In most calibration experiments, all tracks in an 89 mm × 114 mm micrograph of etched cellulose nitrate were counted. Usually, only one determination per sample was made, so there was no direct indication of dispersion, although binomial or Poisson estimates were possible. However, in a few cases, photographs were divided into five sections that were counted separately. The five determinations in each case provided a basis for calculating standard deviations according to the small-sample definition. The results are given in table II. A typical relative deviation was about 10%. Because there were five times as many tracks per determination in calibration experiments, the prediction of dispersion for them should be reduced by a factor of about $1/\sqrt{5}$ to a typical relative deviation of less than 5%. The numbers of tracks per determination listed in the table are, however, directly comparable to the tracks per determination in studies of diffusion profiles to be described later. In either case, the probable error is acceptable, but improvement is desirable. One opportunity for improvement is in developing counting instrumentation to minimise the human factor. Another aid would be the use of plastic detectors especially prepared for this particular service, but they are not available commercially.

2.2. Diffusion

Implementation of the experimental plan depended on the preparation and annealing of diffusion couples of silica and lithium disilicate. Vitreous silica rod of 8 mm diameter and 99.97% purity was used in combination with the H3 material (see table I). Silica melts at 1723° C and lithium disilicate melts in the range 1028 to 1033° C. Several attempts failed to join the materials either as solids or by melting the

TABLE II Track counting uncertainties

Tracks counted* Mean	Standard deviation	Percentile deviation %
82.0	3.0	3.7
73.6	8.1	11.0
71.5	5.8	8.1
67.5	7.1	10.6
61.0	1.9	3.1
58.8	7.8	13.3
45.0	6.6	14.6
41.6	5.2	12.4

* Each sample represents five counts.

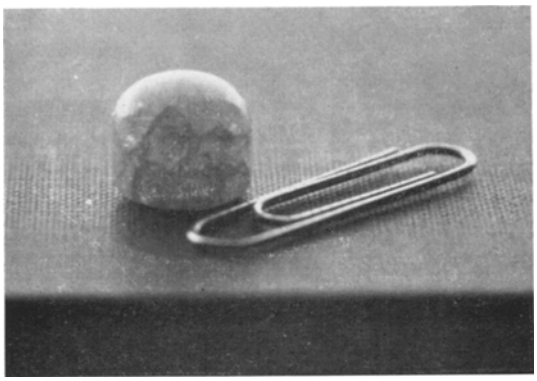

Figure 3 Diffusion couple 031169.

disilicate against solid silica. The main difficulty was a large difference in thermal contraction. Finally, adequate success was achieved by melting lithium disilicate around some of the silica.

A short cylinder of the silica was centred at the bottom of a cylindrical well in a cylindrical crucible of graphite, and broken pieces of lithium disilicate were piled on and around the silica. The bore of the graphite crucible was 13 mm, its wall was 12 mm thick, its height was 10 cm, and the well was 7.5 cm deep. Typically, about 0.75 g of silica and 2.0 g of lithium disilicate were charged, and the mouth of the crucible was covered with graphite foil. The crucible and its contents were heated *in vacuo* by somewhat less than an ampere of electron-bombardment current from a thermionic filament at a potential of several kV. The temperature was monitored by sighting with a disappearing-filament pyrometer into a black-body hole drilled in the crucible wall about 1 cm above the well bottom. The heating power was adjusted to attain a temperature near 1050° C so that the lithium disilicate would be melted around the silica. If the lithium disilicate had been melted in a vacuum previously, it could be resolidified within a few minutes, but if an air-melted glass was used, about an hour of holding time was needed for elimination of dissolved gases (mainly CO_2 and CO). Throughout the melting, the graphite crucible sat on a stool of water-cooled copper. This accelerated freezing when heating was stopped, and cooling was enhanced even more by blowing helium against the crucible after melting was completed. An example of the diffusion couples prepared is shown in fig. 3.

Because of contraction against the silica, the lithium disilicate cracked, but even so a useful

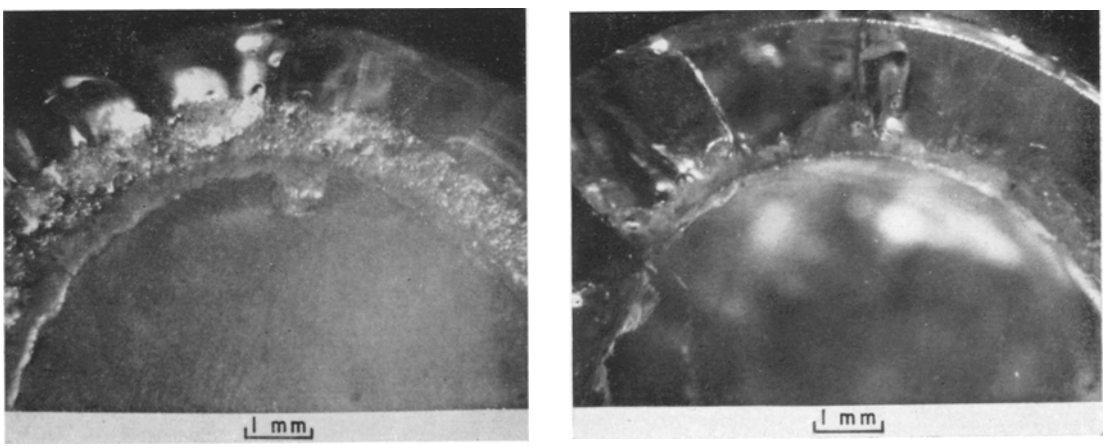

(a) (b)

Figure 4 Joint between glasses, couple 031169, (a) as-cast, (b) after polishing.

bond between materials was obtained around most of the circumference, as shown in fig. 4. Both parts of most couples were clear vitreous materials in the as-cast condition. One such couple was annealed for 186.4 h at about 895° C, autoradiographed, annealed for another 163.9 h at about 880° C, and then autoradiographed once more. Fig. 5 is a view of the joint region after cumulative diffusion for 350.3 h. In this condition, most of the lithium disilicate is devitrified, most of the silica is not, and between them is a band of glassy-appearing, opalescent material.

To test the possibility that a serious interaction between materials had occurred during specimen preparation, three different diffusion couples were autoradiographed in as-cast condition, before diffusion annealing. Corresponding to the interface between materials, each autoradiograph revealed an abrupt drop of the density of alpha tracks from a value representative of lithium disilicate to zero, within a distance of 20 μm. At least part of this apparent thickness was due to the inevitable ejection of some alpha particles at oblique angles from the disilicate side of the junction.

Diffusion annealing was effected in an alumina tube furnace. Argon was bled through the tube during diffusion, and the diffusion couples were nested in silica wool to avoid contact with the alumina. Silica wool was also used as permeable plugs in the tube openings. A Pt–Pt/10% Rh thermocouple was used for temperature measurement.

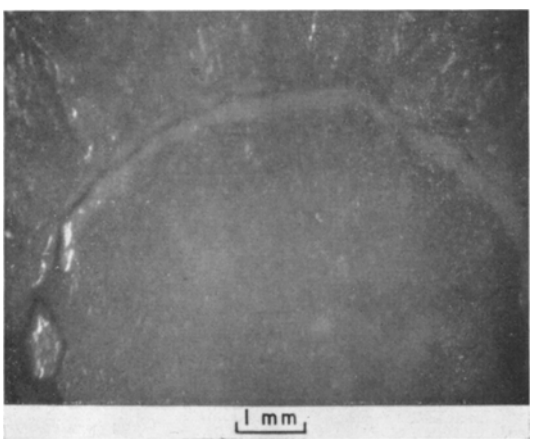

Figure 5 Joint between materials, couple 122867, after diffusion and autoradiography.

3. Experimental Results

Information about the miscibility of lithia in silica was contained in the autoradiographs of the annealed diffusion couple. The autoradiographic procedure was the same as for calibration purposes, except that mosaic sequences of micrographs were obtained along radial directions approximately normal to diffusion interfaces. Adjacent photographs were overlapped slightly so they could be matched to each other according to track patterns. The alpha tracks were counted incrementally in narrow sections of the photo frames, ruled off normal to the diffusion direction. Areal track densities were converted to lithia compositions and plotted on an appropriate scale of distance. The results are presented in figs. 6, 7, and 8. The separate pro-

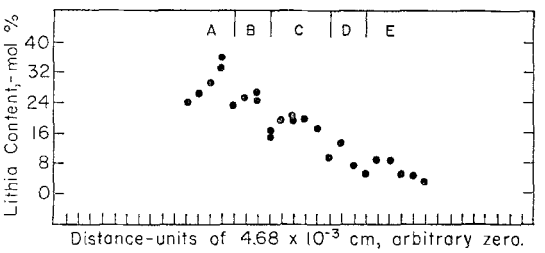

Figure 6 Diffusion-zone profile no. 122867 (4), after 186·4 h at about 895° C.

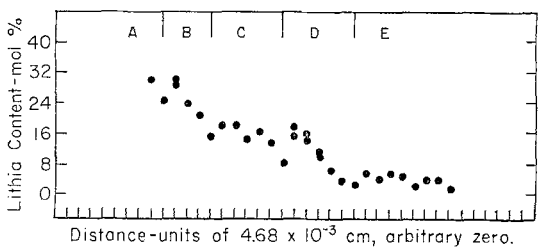

Figure 7 Diffusion-zone profile no. 122867 (5A), after 350·3 h at about 880 to 895° C.

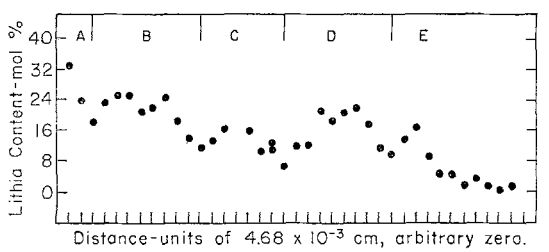

Figure 8 Diffusion-zone profile no. 122867 (5B), after 350·3 h at about 880 to 895° C.

files after 350 h of annealing were obtained along different radial directions. Where the overlap of adjacent micrographs exceeded the width of one of the incremental sections, duplicate compositions are shown for the corresponding profile positions. The largest difference between duplicate values appears near the centre of fig. 7, and it corresponds to a deviation of about 10%, in good agreement with expectations based on table II.

It appears that the diffusion couple was heated too long at 350 h. Phase separations became less distinct by that time because of compositional homogenisation. Nevertheless, each of the diffusion profiles is divisible, at points of relatively low lithia content, into five regions. These are indicated by the letters A to E in the figures. Furthermore, among the separate profiles there is a consistency of the compositional ranges within each region that seems to be more than coincidental. An evaluation of the data on this basis is presented in table III.

4. Discussion

Fig. 9 is a phase diagram for a silica-rich part of the lithia-silica system. The equilibrium boundaries are essentially as reported by Kracek [16] but a metastable liquid–liquid miscibility boundary as calculated by Charles [17] has been superimposed, and other metastable subsolidus features have been added by projecting liquidus boundaries through the eutectic point. Silica and lithium disilicate are the terminal components of the subsystem shown, and in the limit of ideal equilibrium at temperatures below 1028° C, their crystalline polymorphs should be the only phases present. However, all transformations in the system are quite sluggish, so that true equilibrium is rarely if ever approached. Thus, both crystalline and vitreous intermediate phases exist metastably. The regions of metastable crystalline solution are of limited extent near the terminal compositions: probably about 0 to 5 [18-21] and 25 to 33 [22] mol % of lithia. These regions are not shown in fig. 9. Vitreous phases can be formed across the entire subsystem, albeit most readily at compositions exceeding 20 mol % of lithia, and in the central part of the subsystem, they are the only single-phase solids formed. Yet, these glasses all devitrify. Devitrification temperatures for lithium disilicate are generally greater than 500° C, for silica they are generally greater than 1200° C, and most intermediate compositions seem to behave more nearly like the disilicate. The crystallisation or devitrification process presumably involves a shift of composition to the regions where crystalline phases are at least metastable. A prerequisite part of such a shift would be a liquid–liquid phase separation of the initial vitreous composition. This, in part at least, is the essence of the metastable miscibility gap. Indeed, phases may actually be separated on a very finely divided scale in glasses that appear to be single phase as quenched from liquid, and there well may be a spinodal associated with the miscibility boundary.

TABLE III Regional variations of lithia composition* in diffusion profiles

	Profile identification 122867(4) %	122867(5A) %	122867(5B) %	Average %
Region A:				
minimum	26	27	20	25
Region B:				
maximum	29	33	28	30
minimum	16	16	11	15
Region C:				
maximum	24	20	20	21
minimum	11	10	8	10
Region D:				
maximum	15	20	25	20
minimum	6	4	11	7
Region E:				
maximum	10	7	20	11

* Values are mol % of lithia.

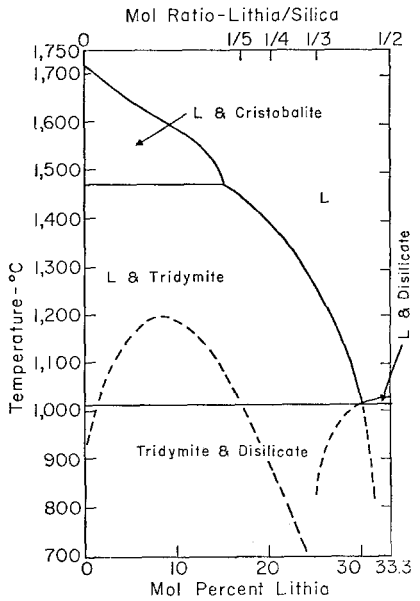

Figure 9 Phase diagram for the subsystem SiO_2-$Li_2O \cdot 2SiO_2$.

Rhines [23] and Cahn [24, 25] have discussed many relevant features inherent in the diffusion behaviour of complex systems. All phases along the diffusion-temperature isotherm of a system should be exhibited in the diffusion profile. However, if a well-behaved system is essentially binary, two-phase regions will appear as discontinuities, and if the system is essentially ternary, three-phase regions will appear as discontinuities. The existence of such discontinuities in diffusion profiles has been well established and the basic reasons for them have been worked out in terms of chemical potentials [26-28]. In addition, negative diffusion coefficients are not unusual in metastable systems, especially those involving a spinodal. These features of behaviour are manifestations of the Gibbs phase rule.

It is difficult and probably a mistake to try to apply the guide-lines too rigorously or too specifically to the diffusion profiles in figs. 6, 7, and 8. The presence of discontinuities can be interpreted fairly as evidence of mixed phases, but because of the highly metastable character of the system, boundaries of neither single- nor two-phase regions are inviolate. Neither is it clear exactly what constitutes a separate phase, except that crystalline material should be distinguished from vitreous matter. Phase regions are not strictly bounded. For example, a phase can readily overlap into a range of compositions that otherwise or elsewhere corresponds to mixed phases. Nevertheless, separate phase regions should tend to extend between some pair of metastable boundaries, even though intermediate boundaries are ignored. Thus, the really important diffusion-profile features are the appearance of phase separations and the recurrence of certain limiting compositions. This viewpoint provides a reasonable basis for explaining some aspects of the diffusion profiles obtained.

Perhaps the situation will be illuminated by citing some superficial similarities with metal systems cooled under non-equilibrium or metastable conditions. However, the analogy must not be carried too far, for there are some fundamental differences. One of the well-known effects of non-equilibrium cooling on metal alloys is the phenomenon of "coring". This occurs during solidification from liquid, but there are comparable events at subsolidus phase boundaries, especially in peritectoid systems. In typical practice, as a particular substance is cooled past an equilibrium boundary, there may not be time for the attainment of equilibrium. Thus the substance "ignores" the equilibrium boundary and responds instead to a virtual boundary that is displaced from the equilibrium position to a metastable position. It was to such limits of metastability that Gibbs originally applied the term "spinodal", and the result is usually a structure somewhat resembling a cored alloy. Now, in principle, the same sort of thing should happen when a specimen is carried across a phase boundary because of a change of composition (viz. by diffusion) instead of a change of temperature. However, in metals, transformations are sufficiently rapid, compared to diffusion, that departures from equilibrium due to this cause are not prominent. In silicate systems, the transformations are very much slower and there is a better chance that the mechanism operates. If it does, random segregation should be expected to some degree, but these features should be superimposed on a layered or banded segregation conforming to the sequence of phase regions in the system, in accordance with the established diffusion behaviour already cited. In metals, non-equilibrium segregated structures are usually undesirable and they are homogenised by heat-treatment. This appears to be what has begun to happen in silica-lithium disilicate diffusion couples heated for 350 h (figs. 7 and 8).

Before proceeding, the likely relationship of a spinodal with the metastable miscibility

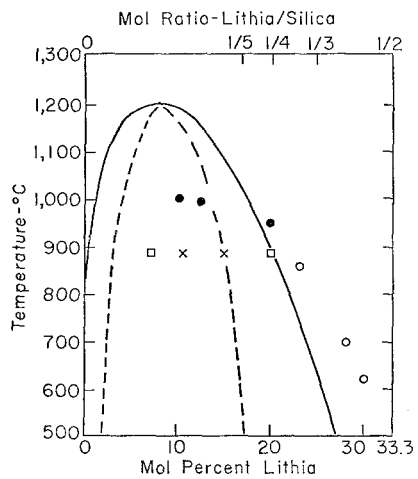

Figure 10 Liquid immiscibility between SiO_2 and $Li_2O \cdot 2SiO_2$; curves from [17], ○ from [29], ● from [30], □ and × from this work; dashed line and ×'s are spinodal estimates.

boundary needs to be fixed a little more definitely. The spinodal was not included in fig. 9, but a predicted spinodal boundary is shown in fig. 10 along with a repetition of the miscibility boundary and some experimental estimates [29, 30] of discrete points on the boundaries, including some values yet to be suggested as a result of this work. The prior experiments were based on the observation that glasses of the system acquire an opalescence under some circumstances, and that this opalescence can be cleared by heating to a fairly definite temperature that depends on the composition of the glass. These clearing temperatures have been taken to lie on the metastable miscibility boundary. Some of the earlier work [30] was done with lithia-silica glasses that contained small amounts of another alkali oxide.

Now, the extended liquidi, the miscibility boundary, and the spinodal boundary are a total of six intermediate metastable boundaries that might cross an isotherm near 885° C. But according to table III, this is just the number of recurring values that seem to be defined by the limits of the regions A to E of the diffusion profiles. It is therefore suggested that there is a direct and appropriately ordered correlation between the indicated values and the expected boundaries. According to this interpretation, the A regions would comprise the devitrified lithium disilicate and its slightly modified crystalline solutions, and the B, C, D, and E regions would be lithium- or lithia-containing glasses. At 885° C, the crystalline solutions apparently persist at compositions down to about 25 mol % lithia, and the glasses overlap this range all the way to the disilicate composition. The complete set of probable boundary values is 7, 11, 16, 20, 25, and 30 mol % of lithia. The first and fourth values are the estimates shown in fig. 10 as miscibility boundary points, and the second and third values are the associated spinodal estimates. The remaining two values possibly are related to the liquidus boundary extensions. It is interesting that the list of proposed boundary values includes compositions near the eutectic (30 mol %), the trisilicate (25 mol %), the tetrasilicate (20 mol %) and the pentasilicate (16.7 mol %).

Results of this work warrant only tentative acceptance. Nevertheless, the implications are a consistent extension of a growing pool of knowledge about the lithia-silica system. The estimates obtained for the lithia-rich sides of the miscibility and spinodal boundaries are in good agreement with predictions based on thermodynamic calculations. On the silica-rich sides of the boundaries, this work provides values somewhat different from the predictions. The one value, on the miscibility boundary, that can be compared with previous experiments agrees fairly well, but not exactly. Overall, the results of experiments seem to indicate an immiscibility region that is narrower, lower, and centred on a composition richer in lithia than the predicted region.

The most reasonable interpretation of results other than that adopted above is that the phase separations apparent in the diffusion profiles are really just random variations about smooth concentration gradients as might be expected from diffusion in an isomorphous system. Implicit in this viewpoint are a rejection of the data presented in table II as an index of the dispersion to be expected in the diffusion profiles of figs. 6 to 8, and a disregard for reports of other experimental experiences including electron microscopy, electrical conductivity measurements, differential thermal analyses, X-ray diffraction, and low-angle X-ray scattering, all of which indicate that a prominent characteristic of silica-lithium disilicate glasses is microscopic heterogeneity. These conflicts make the alternate interpretation even less tenable than the hypothesis of this paper.

5. Summary

Basic guidelines and groundwork for improve-

ment were established for applications of neutron-induced autoradiography, especially in ceramography of lithium-bearing substances. Worthwhile capabilities were thereby demonstrated for materials research. In specific relationship to the lithia-silica system, neutron-induced autoradiography of diffusion profiles contained interesting information about the metastability of both glasses and ceramics. Points were tentatively evaluated on miscibility and spinodal boundaries. The agreement with prior evidence was reasonable for compositions rich in lithium disilicate, but poor for silica-rich compositions.

Acknowledgement

This disclosure is based on a thesis submitted to Oregon State University, prepared as a part of National Science Foundation Grant GK-2043. However, most of the specimen preparation and diffusion couple annealing were done in apparatus located at the Albany Metallurgy Research Center of the U S Bureau of Mines. The Bureau's staff also contributed samples of appropriate glasses. These contributions are deeply appreciated.

References

1. C. P. BEAN, R. L. FLEISCHER, P. W. SWARTZ, and H. R. HART JR., *J. Appl. Phys.* **37** (1966) 2218.
2. J. S. ARMIJO and H. S. ROSENBAUM, *ibid* **38** (1967) 2064.
3. N. A. TINER, T. L. MACKAY, S. K. ASUNMAA, and R. G. INGERSOLL, *Trans. ASM* **61** (1968) 195.
4. H. S. ROSENBAUM and J. S. ARMIJO, *J. Nucl. Matls.*, **22** (1967) 115.
5. J. D. KLEEMAN and J. F. LOVERING, *Science* **156** (1967) 512.
6. G. AMSEL and D. SAMUEL, *J. Phys. Chem. Solids* **23** (1962) 1707.
7. R. W. OLLERHEAD, E. ALMQVIST, and J. A. KUEHNER, *J. Appl. Phys.* **37** (1966) 2440.
8. G. AMSEL, G. BÉRANGER, B. DE GÉLAS, and P. LACOMBE, *ibid* **39** (1968) 2246.
9. R. L. FLEISCHER, P. B. PRICE, and R. M. WALKER, *Phys. Rev.* **133** (1964) A1443.
10. P. B. PRICE and R. M. WALKER, *J. Appl. Phys.* **33** (1962) 3400.
11. *Idem, ibid* 3407.
12. R. L. FLEISCHER, P. B. PRICE, and R. M. WALKER, *Rev. Sci. Instr.* **37** (1966) 525.
13. J. H. DAVIES and R. W. DARMITZEL, *Nucleonics* **23** (1965) 86.
14. E. V. BENTON, US Naval Radiological Defense Lab., Rept. TR-68-14, San Francisco, 1968; Defense Doc. Center No. AD 666543.
15. J. I. PAIGE, H. M. HARRIS, and H. J. KELLY, US Bureau of Mines, Rept. RI 6651, Washington, DC, 1965.
16. F. C. KRACEK, *J. Phys. Chem.* **34** (1930) 2641.
17. R. J. CHARLES, *J. Amer. Ceram. Soc.* **50** (1967) 631.
18. M. J. BUERGER, *Zeits. Krist.* **90** (1935) 186.
19. *Idem, Am. Mineral.* **39** (1954) 600.
20. *Idem, Fortschr. Mineral.* **39** (1961) 4.
21. R. B. SOSMAN, "The Phases of Silica" (Rutgers Univ. Press, New Brunswick, New Jersey, 1965) p. 56.
22. F. P. GLASSER, *Phys. and Chem. of Glasses* **8** (Dec. 1967) 224.
23. F. N. RHINES, in "Surface Treatment of Metals" (Am. Soc. for Metals, Metals Park, Ohio, 1941) p. 123.
24. J. W. CAHN, *J. Chem. Phys.* **42** (1965) 93.
25. *Idem, Trans. AIME* **242** (1968) 166.
26. L. S. DARKEN, *ibid* **180** (1949) 430.
27. *Idem*, in "Atom Movements" (Am. Soc. for Metals, Metals Park, Ohio, 1951) pp. 20-23.
28. W. JOST, "Diffusion in Solids, Liquids, Gases" (Academic Press, New York, 1952) pp. 68-77 and 160-163.
29. N. S. ANDREEV, D. A. GOGANOV, E. A. PORAI-KOSHITS, and YU. G. SOKOLOV, in "The Structure of Glass, vol. 3. Catalyzed Crystallisation of Glass" (Consultants Bureau, New York, 1964) p. 47.
30. Y. MORIYA, D. H. WARRINGTON, and R. W. DOUGLAS, *Phys. and Chem. of Glasses* **8** (Feb. 1967) 19.

Received 24 November 1969 and accepted 23 February 1970.